Translational Oncology 45 (2024) 101988

Contents lists available at ScienceDirect

Translational Oncology

journal homepage: www.elsevier.com/locate/tranon

Original Research

Fractionated radiation therapy alters energy metabolism and induces cellular quiescence exit in patient-derived orthotopic xenograft models of high-grade glioma

Zi-Lu Huang [a,b,1], Zhi-Gang Liu [c,d,e,1,*], Qi Lin [b,f], Ya-Lan Tao [a], Xinzhuoyun Li [b], Patricia Baxter [e], Jack MF Su [e], Adekunle M. Adesina [g], Chris Man [e], Murali Chintagumpala [e], Wan Yee Teo [e,h,i], Yu-Chen Du [b,e,j,**], Yun-Fei Xia [a,***], Xiao-Nan Li [b,e,j,**]

[a] Department of Radiation Oncology, State Key Laboratory of Oncology in South China, Guangdong Provincial Clinical Research Center for Cancer, Sun Yat-Sen University Cancer Center, Guangzhou 510060, PR China
[b] Department of Pediatrics, Program of Precision Medicine PDOX Modeling of Pediatric Tumors, Ann & Robert H. Lurie Children's Hospital of Chicago, Northwestern University Feinberg School of Medicine, Chicago, IL 60611, United States
[c] Cancer Center, The 10th Affiliated Hospital of Southern Medical University (Dongguan People's Hospital), Southern Medical University, China
[d] Dongguan Key Laboratory of Precision Diagnosis and Treatment for Tumors, The 10th Affiliated Hospital of Southern Medical University, Southern Medical University, China
[e] Texas Children's Cancer Center and Department of Pediatrics, Baylor College of Medicine, Houston, TX, United States
[f] Department of Pharmacology, School of Medicine, Sun Yat-Sen University, Guangzhou, Guangdong 510080, China
[g] Department of Pathology, Texas Children's Hospital, Houston, TX, United States
[h] The Laboratory of Pediatric Brain Tumor Research Office, SingHealth Duke-NUS Academic Medical Center, 169856, Singapore
[i] Cancer and Stem Cell Biology Program, Duke-NUS Medical School Singapore, A*STAR, KK Women's & Children's Hospital Singapore, Institute of Molecular and Cell Biology, Singapore
[j] Robert H. Lurie Comprehensive Cancer Center, Northwestern University Feinberg School of Medicine, Chicago, IL 60611, United States

ARTICLE INFO

Keywords:
Mitochondrial biogenesis
Radiotherapy
Orthotopic xenograft
Glioma
Cancer stem cells

ABSTRACT

Radiation is one of the standard therapies for pediatric high-grade glioma (pHGG), of which the prognosis remains poor. To gain an in-depth understanding of biological consequences beyond the classic DNA damage, we treated 9 patient-derived orthotopic xenograft (PDOX) models, including one with DNA mismatch repair (MMR) deficiency, with fractionated radiations (2 Gy/day x 5 days). Extension of survival time was noted in 5 PDOX models ($P < 0.05$) accompanied by γH2AX positivity in >95 % tumor cells in tumor core and >85 % in the invasive foci as well as ~30 % apoptotic and mitotic catastrophic cell death. The model with DNA MMR (IC-1406HGG) was the most responsive to radiation with a reduction of Ki-67(+) cells. Altered metabolism, including mitochondria number elevation, COX IV activation and reactive oxygen species accumulation, were detected together with the enrichment of $CD133^+$ tumor cells. The latter was caused by the entry of quiescent G_0 cells into cell cycle and the activation of self-renewal (SOX2 and BMI1) and epithelial mesenchymal transition (fibronectin) genes. These novel insights about the cellular and molecular mechanisms of fractionated radiation *in vivo* should support the development of new radio-sensitizing therapies.

Abbreviations: pHGG, pediatric glioblastoma multiforme; IC, intracerebral; SCID, severe complex immunodeficiency; CSC, cancer stem cell; MT, mitochondria; ROS, reactive oxygen species; MMR, mismatch repair.

* Corresponding author at: Cancer Center, The 10th Affiliated Hospital of Southern Medical University (Dongguan People's Hospital), Southern Medical University, China.

** Corresponding authors at: Department of Pediatrics, Program of Precision Medicine PDOX Modeling of Pediatric Tumors, Ann & Robert H. Lurie Children's Hospital of Chicago, Northwestern University Feinberg School of Medicine, Chicago, IL 60611, United States.

*** Corresponding author at: Department of Radiation Oncology, State Key Laboratory of Oncology in South China, Guangdong Provincial Clinical Research Center for Cancer, Sun Yat-Sen University Cancer Center, Guangzhou 510060, PR China.

E-mail addresses: liuzhigang1983@smu.edu.cn (Z.-G. Liu), yuchdu@luriechildrens.org (Y.-C. Du), xiayf@sysucc.org.cn (Y.-F. Xia), xiaonan.li@northwestern.edu (X.-N. Li).

[1] These authors contributed equally to this work.

https://doi.org/10.1016/j.tranon.2024.101988
Received 29 November 2023; Received in revised form 23 April 2024; Accepted 6 May 2024
Available online 10 May 2024

Introduction

Pediatric high-grade glioma (pHGG), previously termed as glioblastoma (GBM), is one of the most lethal brain malignancies that occurs in children with a 3-year survival of less than 20 % [1–4]. Diffuse invasion invariably impedes a curative tumor resection. However, the development of resistance to radiation, the most important standard therapy administered to nearly all pHGG patients, is one of the main causes of tumor recurrence ([5,6]). Improved understanding of the molecular mechanisms of radio-resistance of pHGG is needed, particularly *in vivo* and after treatment with clinically relevant fractionated radiation.

Genomic DNA has long been recognized as the prime subcellular target of radiation therapy, and DNA damage repair represents one of the major mechanisms of tumor cell survival [7–9]. For pHGGs, however, there are still several fundamental questions that remain to be answered. First, does radiation cause identical DNA damages in both tumor core and in invasive cells? Invasive cells are often surrounded by normal brain cells in a microenvironment that is different from the tumor core area. Secondly, are there additional mechanisms supporting the survival of irradiated pHGG cells? If pHGG cells have additional survival mechanisms, simple suppression of DNA repair may have limited efficacy because these tumor cells will adopt alternative mechanisms to overcome cell death. Indeed, emerging data suggest that mitochondria, the primary source of energy supply and key player in multiple cell death pathways [10], might be involved in radio-resistance. Since mitochondrial biogenesis and oxidative metabolism can be stimulated in response to pathological stress [11], we hypothesize that radiation would trigger mitochondrial biogenesis *in vivo* to promote tumor cell survival.

There is compelling evidence that cancer stem cells (CSCs) contribute to radiation resistance [12]. Many solid cancers are organized hierarchically and contain a small population of CSCs that possess strong self-renewal and multi-differentiation capacities. Several key self-renewal regulators, including SOX2 and BMI1 that are highly expressed in pHGG tumors ([13,14]), and genes involved in epithelial-mesenchymal transition (EMT) [10] are shown to mediate radio-resistance in human cancers [11]. Enhanced DNA repair capacity has been detected in adult GBM stem cells, and fractionated radiotherapy was also found to enrich CSCs in breast tumor [15]. However, the cause of post-radiation CSC enrichment remains poorly elucidated. While quiescent (G_0 phase) CSC subpopulation is thought to be resistant to radiation [16], the impact of radiation on the fate of quiescent CSCs has not been fully investigated.

Microenvironment plays an important role in regulating radiosensitivity of human cancers [17]. Through direct injection of fresh surgical specimens into anatomically matched locations in the brains of SCID mice, we have established a panel of patient-derived orthotopic xenograft (PDOX) mouse models for pediatric brain tumors [18–20]. These xenograft tumors replicated the histopathological phenotypes, maintained major genetic abnormalities [20], preserved CSC pool, and reproduced the diffuse invasive growth patterns of the original patient tumors. One of the newly established glioma models was derived from a patient with Turcot's syndrome with confirmed mutation of PMS2, a gene involved in DNA mismatch repair (MMR) ([21,22]). Herein, we described our *in vivo* examination of therapy efficacy of fractionated radiations in a panel of 9 PDOX models and our effort to understand radio-resistance mechanisms of pHGGs by employing clinically relevant fractionated radiation treatment. To estimate the contributions of DNA repair on radiation resistance and the role of mitochondrial biogenesis, we compared the biological responses of a DNA MMR deficient model (IC-1406pHGG) with that of a DNA repair competent model (IC-2305pHGG). The impact of radiation on putative CSCs, particularly on the quiescent $CD133^+$ tumor cells, were subsequently analyzed with key genes of self-renewal and EMT *in vivo* in two additional PDOX models.

Materials and methods

Tumor tissues

Fresh tumor tissues were obtained from 9 children who underwent craniotomy in Texas Children's Hospital (Table 1) following informed consent to an Institutional Review Board (IRB) of Baylor College of Medicine approved tissue bank protocol ([18,19]). Tumor tissues collected from the cryostat laboratory were quickly transferred in DMEM growth medium supplemented with 10 % FBS on ice to the tissue culture room, where they were washed and mechanically dispersed. After the cell suspension was passed through a 35 μ cell strainer, the live tumor cells as single cells and small clumps (~5–10 cells) were counted with trypan blue staining, resuspended in growth medium (1×10^8/mL), and transferred to animal facility on ice.

Orthotopic transplantation into the brains of SCID mice

Surgical transplantation of tumor cells into mouse cerebrum was performed as we described previously ([18,19]), following the Institutional Animal Care and Use Committee (IACUC) approved protocol at Baylor College of Medicine and Northwestern University. Two strains of SCID mice were used. The Rag2/SCID mice that have exhibited high tumor take rate (> 55 %) in our previous studies were used for the initial establishment of xenografts. For the *in vivo* treatment with radiation, the NOD.129S7 (B6)-Rag1tm1Mom/J (stock number 003729) SCID mice (Jackson Lab, Bar Harbor, Maine), which can tolerate radiation ([23,24]), were adopted. These mice were bred and maintained in a specific pathogen free animal facility. Mice, aged 6–8 weeks of both sex, were anesthetized with sodium pentobarbital (50 mg/Kg). Tumor cells (1×10^5) were suspended in 2 μL of culture medium and injected into the cerebral hemisphere (1 mm to the right of the midline, 1.5 mm anterior to the lambdoid suture and 3 mm deep) via a 10 μL 26-gauge Hamilton Gastight 1701 syringe needle. Animals were monitored daily and those that developed signs of neurological deficit or became moribund were euthanized and had their brains removed for histopathological analysis or tumors harvested for *in vivo* subtransplantation. To perform serial subtransplantations in mouse brain, whole brains of the donor mice

Table 1
List of PDOX mouse models of pediatric high-grade glioma.

MODEL ID	AGE/GENDER	PASSAGE *IN VIVO*	MOLECULAR SUBTYPE	GFAP	P53	KI-67	MUTATION
IC-1406HGG	5 Y/F	8	UNCLEAR	+	+4	4	PMS2(S46I) (TURCOT'S SYNDROME)
IC-2305HGG	9 y/M	6	G34	+	+3	4	TP53, H3F3A(G35R), ATRX
IC-3752HGG	5 y/F	8	MYCN	+++	NA	NA	WNT6, STAT1, ERCC8, DDX46
IC-1128HGG	8.7 y/M	8	MYCN	+++	+	NA	R342X, PIK3CA, TP73, TP53, RB1, NF1
IC-10993HGG	11 y/M	4	pedRTKIa	NA			
IC-2583HGG	NA	4	pedRTK1a	NA			
IC-3704HGG	12 y/M	6	pedRTKIII	+++	+	2	SYFU, PR3R1
IC-8100HGG	14 y/M	4	DMG_K27	NA			

Note: Intensity of staining: +: weak; ++: moderate; +++: strong; Percentage: 1=<25 %, 2=25–50 %, 3=50–75 %, 4=>75 % MYCN: V-myc myelocytomatosis viral-related oncogene. G34: glycine 34 to either arginine, G34R, or valine, G34V. RTK III: termed receptor tyrosine kinase III. RTK Ia: termed receptor tyrosine kinase Ia.

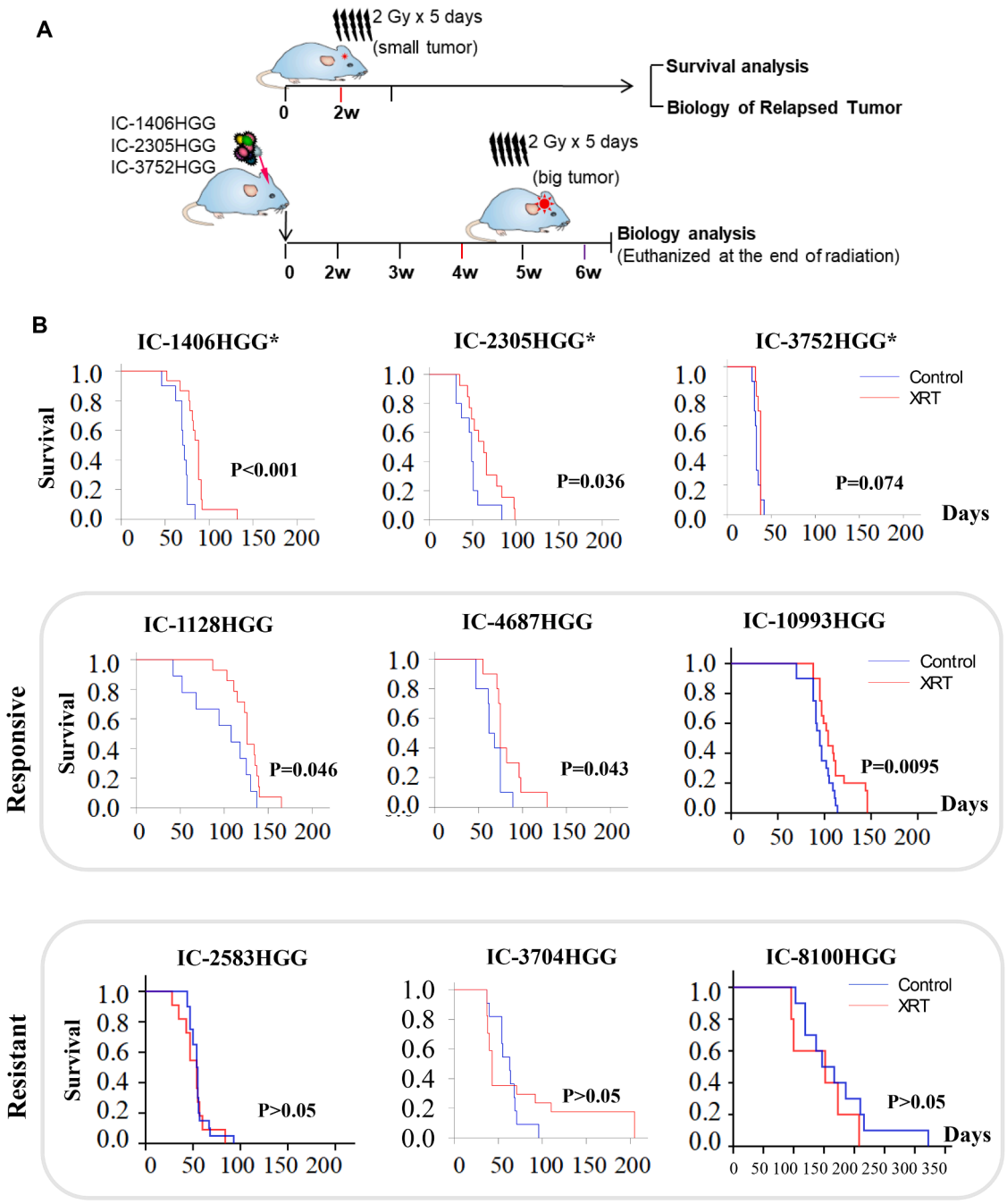

Fig. 1. *In vivo* treatment of PDOX models of pHGG with fractionated radiotherapy. (A) Experiment design of the study. Tumor cells (1×10^5 cells/2 μL) were implanted into right cerebral cortex of SCID mice. Fractionated radiation (2 Gy/day x 5 days) was administered 14 days and ~5 weeks post tumor implantation for survival analysis and for biological examination, respectively. (B) Log rank analysis of animal survival times in 6 pHGG models. There were at least 10 mice for each control and radiation therapy (XRT) group. The model marked with * were selected in this research for further biological verify and analysis.

were aseptically removed and transferred back to tissue culture laboratory where the tumors were dissected out of the surrounding normal brain tissues and made into single cell suspensions. Tumor cells were then counted and injected (1×10^5 cells/mouse) into the brains of the recipient SCID mice ([18,19,25]).

PMS2 sequence analysis

ST-1406HGG was derived from a child with Turcot's syndrome carrying a c.137G>T (p.S46I) mutation in PMS2 gene. Targeted sequence analysis for this mutation in xenograft tumor of IC-1406HGG was performed by the Medical Genetics Laboratories at Baylor College of Medicine. Briefly, genomic DNA was extracted with DNeasy (Qiagen). A PCR-based assay was used to amplify the exon in which the familial mutation is located. The amplified product was sequenced in both the forward and reverse directions using automated fluorescence dideoxy sequencing methods. Reference sequences NM_000535.5 and NG_008466.1 were used for sequence comparison.

Fractionated irradiation of pre-established orthotopic xenograft tumor

Radiation (118 cGy/min) was administered with RS-2000 Biological irradiator (Rad Source Technologies, Alpharetta, GA). X-Rays were delivered to the xenograft tumors with a custom-made lead shield

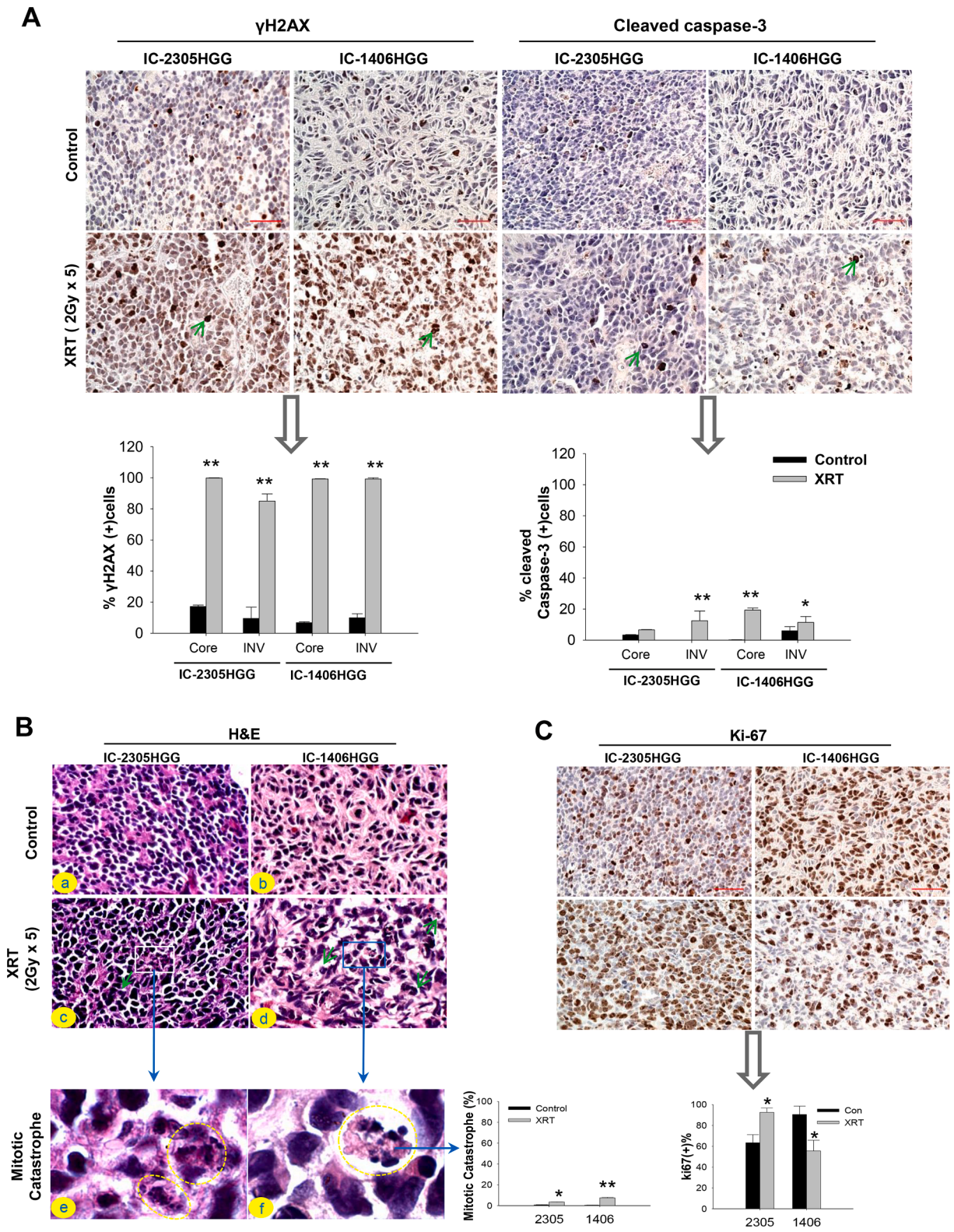

Fig. 2. *In vivo* responses of pHGG tumor cells toward fractionated radiation. (A) Representative images showing the detection of tumor cells with double strand breaks and apoptosis with immunohistochemical staining of γH2AX (*green arrows)* (*left panel*) and cleaved caspase-3 (*green arrows)* (*right panel*), respectively (Bar = 50 μm). Positive cells were counted from at least 5 microscopic fields (10×40) in the tumor core (***Core***) or in at least 8 invasive foci (***INV***) (5–30 cells), and represent as Mean ± SE in the graphs (*lower panel*), ** $P < 0.01$; * $P < 0.05$, compared with the untreated control group. (B) Representative images of H&E staining showing increased volume of cancer cells, cavity formation, nuclear heterogeneity, cell degeneration, cytoplasm dyeing change could be seen (a–d) and sings of mitotic catastrophe (*green arrows and circles*) (c–f) *in vivo* in xenograft tumors treated with or without radiation (2 Gy daily for 5 days). Quantitative data were graphed. (C) Changes of cell proliferation as detected by immunostaining of Ki-67 (*red arrows)* (bar = 50 μm). Mitotic catastrophe and Ki-67 positive cells were counted in at least 5 microscopic fields (10×40) (Mean ± SE), ** $P < 0.01$; *$P < 0.05$, compared with control group. Magnification, 10×40: a–d;10×100: e and f.

through a specially designed hole that is ~2 mm bigger (in diameter) than the intra-cerebral xenograft tumors ([23,24]). Mice in the radiation groups were irradiated 2 Gy daily over 5 consecutive days. The rest of animal body was protected by the lead shield.

Immunohistochemical staining

Immunostaining was performed on paraffin sections using a Vectastain Elite Kit (Vector Laboratories) as described previously ([18,19,24,25]). Primary antibodies included monoclonal antibodies against γ-H2AX (1:100; Cell Signaling), Ki-67 (1:100; Santa Cruz), cleaved caspase-3(1:100; Cell signaling), human mitochondria (MT) (1:50; Abcam), COX IV (1:2000; Cell signaling), BMI1 (1:100, Upstate Cell Signaling Solutions), SOX2 (1:100, Cell Signaling), Fibronectin (1:150, BD Bioscience) and Vimentin (1:200, Dako). The information recorded included the intensity of staining (graded 0, negative; +, weak; ++, moderate; and +++, strong) and the percentage of positive cells (0–100 %). Quantitation of positive cells in the tumor core area was performed on digital images using ImageJ, and in the invasive cells through direct count of positive cells in at least 8 micro-invasive foci (5–30 cells).

Flow cytometric analysis of cell surface marker

Xenograft cells (1×10^6) were incubated with fluorochrome-conjugated antibodies for 15–30 min at 4 °C in 100 μL of Hanks' balanced saline solution (HBSS) containing 2 % FBS and 5–20 μL of each undiluted antibody as we described previously [26–30]. After washing three times in HBSS, cells were suspended in HBSS supplemented with 5 % FBS and subsequently analyzed with a LSR II (Becton Dickinson). The following antibodies were used: CD133-APC (1:10, Milteny Bio, Inc., Auburn, CA).

Flow cytometric analysis of quiescent (G_0) and proliferating cells

Xenograft tumor cells were resuspended in 1 ml DMEM with 100 μM Verapamil (Sigma) and incubation with 10 ug/ml Hoechst33342 (Sigma) at 37 °C for 45 min to stain DNA, followed by incubation with 0.5 mg/mL Pyronin Y to stain RNA, and analyzed with flow cytometer LSRII. Cell cycle was determined by the combined intensity of DNA and RNA, i.e. G_0 (RNA^{low}/DNA^{2n}), G_1 (RNA^{high}/DNA^{2n}), S ($RNA^{high}/DNA^{2n\text{-}4n}$), G_2/M (RNA^{high}/DNA^{4n}).

Flow cytometric analysis of intracellular reactive oxygen species (ROS)

To determine the ROS levels, xenograft cells were incubated with 5 μM 2'-7'-Dichlorodihydrofluorescein diacetate DCF-DA (Invitrogen) at 37 °C for 30 min and analyzed with flow cytometry using LSRII (Becton-Dickinson). Dead cells were gated out through PI staining.

Statistical analysis

Data were presented in graphical form as the mean ± SD or mean ± SE. Changes of animal survival times were analyzed through log-rank analysis. Differences of DNA damage (γH2AX), mitotic catastrophe, cell proliferation (Ki-67 positivity), cell apoptosis (cleaved caspase-3 positivity) between the radiation–treated and control groups were analyzed using student *t* test or one way ANOVA using Sigmaplot 14 ([24,30,31]). Significance was assessed at $P < 0.05$.

Results

In vivo therapeutic efficacy of fractionated radiation

To examine the feasibility of administering clinically relevant radiation therapy, evaluate its efficacy and correlate with overall responses in pHGG patients, SCID mice bearing pre-established orthotopic xenograft tumors at passage III ($n = 10$ per group) were treated with radiation at 2 Gy per day for 5 consecutive days, a regime that closely resembles clinical practice [32]. A total of 9 PDOX models were included (Table 1), many of them have been previously characterized and involved in biological studies and preclinical drug testing ([18,24,28,33,34]). Compared with the untreated control, fractionated radiation prolonged the median survival time in 5/9 PDOX models ($P < 0.05$) with the DNA mismatch repair (MMR) deficiency model IC-1406HGG, which bears a c.137G>T (p.S46I) mutation in PMS2 gene that was originally detected in the patient tumor, as the most responsive ($P < 0.001$, Fig. 1A,B). The animal survival times were extended ~ 10 %. These data showed inter-tumoral heterogeneities toward fractionated radiation in pHGG PDOX models and overall similar efficacy to pHGG patients in clinic.

Fractionated radiation caused wide-spread DNA damage in vivo in pHGG cells

DNA is the primary target for cell damage following ionizing radiation [8]. To examine the role of DNA damage and repair in radiation-induced cell-killing *in vivo* and to assess the activity of fractionated radiation, we selected two PDOX models with (IC-1046HGG) and without (IC-2305HGG) DNA MMR deficiency. We treated animals with preformed orthotopic xenograft tumors (~ 8–10 mm in diameter) approximately 5 weeks post tumor implantation (Fig. 1A) with fractionated radiation at 2 Gy daily dose for 5 days [32]. At the end of treatment, DNA damage was evaluated through immunohistochemical staining of phosphorylated histone H2AX (γH2AX), which selectively accumulates in double strand breaks ([35,36]), on paraffin sections of whole mouse brains. As show in Fig. 2A, γH2AX expression was significantly increased in the core areas of radiation treated xenograft tumors and nearly all tumor cells (>98 %) were stained low to medium (+ ~ ++) in IC-2305HGG, and medium to high (++ ~+++) in the DNA MMR deficient IC-1406HGG, indicating that the fractionated radiation was effective in causing DNA breaks *in vivo* and tumors with DNA MMR deficiency were more sensitive to radiation induced DNA damage.

Diffuse invasion is one of the hallmarks of pHGG [37]. To examine if the cells in the invasive foci were equally responsive to radiation induced DNA damage, we compared the extent of DNA breaks in the invasive foci with that in the tumor core. Since it is not straightforward to positively distinguish single invasive tumor cells from normal mouse brain cells by morphology, we focused on the micro-invasive foci (between 5 and 30 cells) that can be easily identified. Our results showed that irradiation caused substantial increase of γH2AX positivity in the invasive cells as well, resulting in 85 % ± 4.6 % positivity in IC-2305HGG and 99.8 % ± 0.2 % positivity in IC-1406HGG (Fig. 2**A**). The differences between tumor core and their corresponding invasive foci were not significant ($P > 0.05$). These data suggested that the invasive cells shared similar susceptibility toward radiation induced DNA damages as the tumor core cells. They also showed that the radiation fields on our mouse models were large enough to cover the orthotopic xenografts.

Radiation induced apoptosis

To examine if DNA damages caused tumor cell apoptosis, we examined the expression of cleaved caspase-3 in the consecutive sections next to the ones used for γH2AX immunostaining in the two PDOX models. In the tumor core area, although there appeared to be an increase of apoptotic cells in the radiation-treated tumor cells as compared with the untreated control, the absolute number of cells in apoptosis was not high (< 10 % in IC-2305HGG and ~ 20 % in IC-1406HGG) (Fig. 2A). Similarly, low levels of cleaved caspase-3 positivity were observed in the invasive foci, suggesting that many tumor cells that suffered DNA damage (demonstrated by elevated γH2AX positivity) in the tumor core and in the invasive foci did not transit into apoptosis.

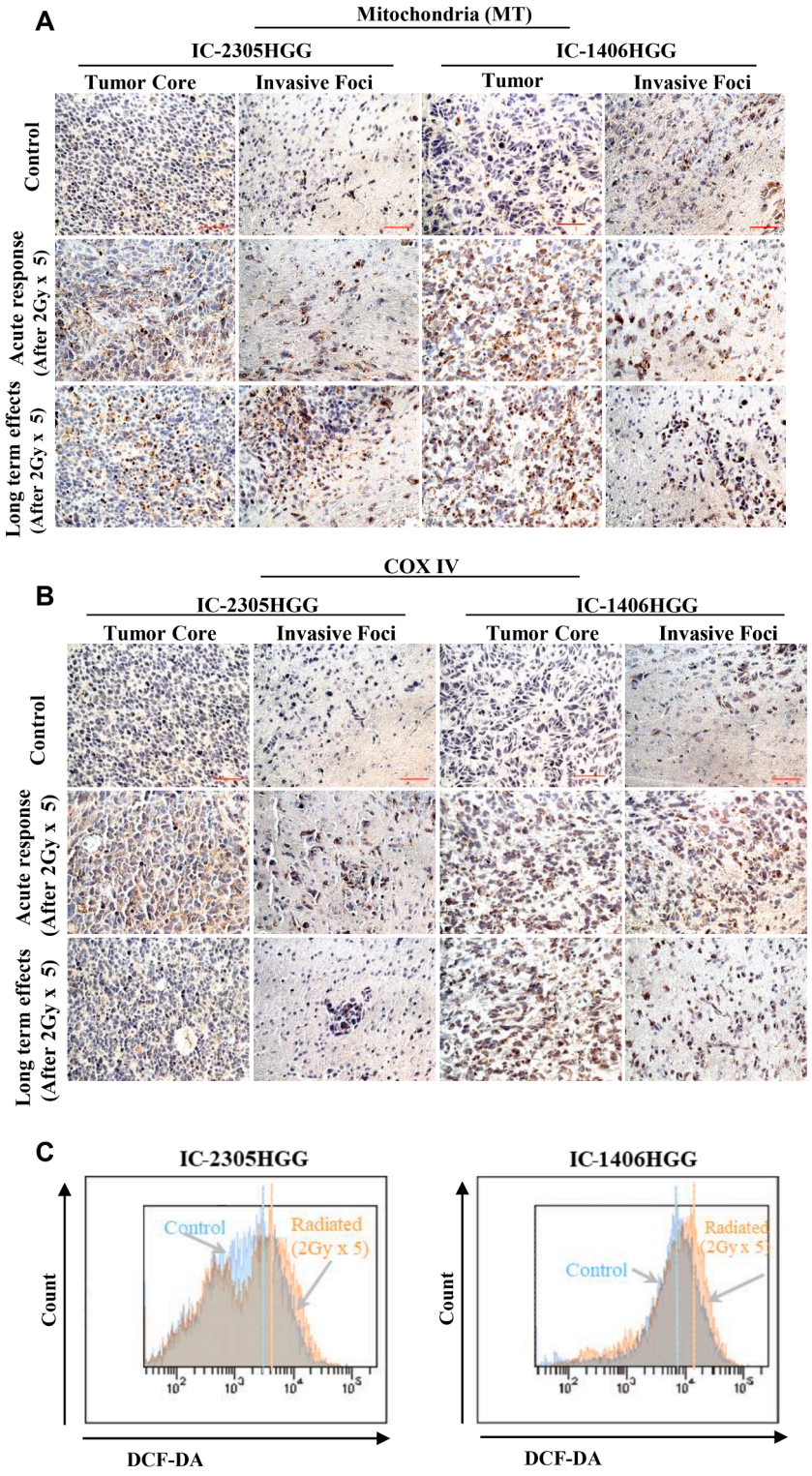

Fig. 3. Representative images of immunohistochemical detection and functional examination of mitochondria *in vivo* in xenograft tumors (quantification data summarized in Table 2). (A) Analysis of mitochondrial abundance in tumor core and invasive foci with immunohistochemical staining. Xenograft tumors harvested immediately at the end of fractionated radiation therapy (***Acute response)*** and at the late phase after fractionated radiation therapy (***Long term effects***) were compared with that in the untreated control group. bar = 50 μm. (B) Immunohistochemical staining of mitochondria-specific protein COX IV. Xenograft tumors harvested immediately at the end of fractionated radiation therapy (***Acute response)*** and at the late phase after fractionated radiation therapy (***Long term effects***) were compared with the untreated control, bar = 50 μm. **(C)** FCM quantitative analysis of ROS production. Xenograft cells were harvested at the end of 5-day fractionated radiation, stained with DCF-DA and analyzed.

Fractionated radiation caused mitotic catastrophe

Mitotic catastrophe, the process when cells tend to divide without proper repair of DNA damage, was shown to be a mechanism of radiation-induced cell death [38]. To evaluate the impact of mitotic catastrophe, we examined the characteristic morphological changes of mitotic catastrophe, i.e. the multiple micronuclei, nuclear fragmentation and aberrant segregation of chromatids [38], on H&E stained sections derived from animals after the 5-day radiotherapy. In IC-2305HGG, mitotic catastrophe increased from 0.6 % ± 0.5 % in the control group to 3.4 % ± 0.4 % (5.6-fold increase) in the irradiated cells (Fig. 2B) ($P < 0.05$); whereas in IC-1406HGG (the model with DNA MMR deficiency), cells in mitotic catastrophe increased from 0.4 % ± 0.3 % to 7.3 % ± 0.8 % (18.3-fold increase) after fractionated radiation (Fig. 2B) ($P < 0.01$), highlighting mitotic catastrophe as one of the mechanisms of radiation-induced cell-killing in pHGGs.

Previous reports showed that ionizing radiation also caused morphological changes of tumor cells *in vitro* and *in vivo* ([39,40]). In this study, examination of H&E stained sections following radiation revealed reduced cellular density, increased cytoplasm/nuclear ratio, bizarre pleomorphic cells with occasional multinucleated tumor giant cells and severe cytoplasmic degeneration (Fig. 2B). Similar to DNA damage and apoptosis, IC-1406HGG tumors underwent a more pronounced morphological restructuring than that in the IC-2305HGG xenografts.

Differential impact on cell proliferation in PDOX models with and without DNA MMR deficiency

Changes of cell proliferation of human solid tumors during radiation therapy remain poorly understood, although transient increase in growth faction has been observed in salivary gland neoplasm xenografts and in cervical cancer patients ([41,42]). To determine the impact of radiation on pHGG cell proliferation, we examined the changes of Ki-67, a marker of cell proliferation, through IHC staining. A significant reduction of Ki-67 positive cells from 90 % ± 8 % to 55 % ± 10 % was observed in IC-1406HGG, the model with DNA MMR deficiency (Fig. 2**C**) ($P < 0.05$); whereas in IC-2305HGG, Ki-67 positive cells increased from 62.4 % ± 7.6 % in the untreated tumor to more than 92.5 % ± 4.1 % immediately at the end of the 5-day radiotherapy (Fig. 2**C**) ($P < 0.05$). These findings are interesting as they revealed that pHGG cells activated cell proliferation as an alternative response to radiation-induced stress/damage, except when they harbor DNA MMR deficiency. Since many chemotherapy agents have been successfully developed to target rapid proliferating cells, this finding provided mechanistic rationale to support the combination of radiation with cell-cycle specific chemotherapies.

Mitochondria quantities increased significantly in the surviving tumor cells

Mitochondria play an important role in tumor cell survival and apoptosis ([43,44]). Since some tumor cells survived despite wide-spread DNA damage in both pHGG models, we sought to examine if the surviving cells exhibited signs of mitochondria activation through immunohistochemical staining using human-specific antibodies against mitochondria ([18,19]). In the untreated control group, majority of the tumor cells were mitochondria negative with low levels (+) of positivity in a small fraction (< 10 %) of cells in the tumor mass in both models (Fig. 3A, Table 2). This result is different from our medulloblastoma models, in which nearly all the tumor cells, even in the center of massive xenografts, were richly stained with mitochondria [18]. In contrast, most of tumor cells (70–75 %) in the invasive foci exhibited high (+++) levels of mitochondria positivity, suggesting that oxidative phosphorylation might have played a more important role in the invasive cells. It also highlighted a substantial metabolic difference between the tumor core and invasive pHGG cells *in vivo*. In the xenograft tumors that were treated with fractionated radiation (2 Gy daily for 5 days), a significant increase of strong mitochondria positivity (+++) was detected in tumor mass (80 % in IC-2305HGG and 95 % in IC-1406HGG) and in nearly all tumor cells (90 % in IC-2305HGG and 95 % in IC-1406HGG) in the invasive front (Fig. 3A, Table 2).

Table 2
Summary for immunohistochemical detection of mitochondrial related proteins.

Gene	Group	IC-2305HGG		IC-1406HGG	
		Tumor Core	Invasive Foci	Tumor Core	Invasive Foci
MT	Control	+, 10 %	++, 70 %	+, 5 %	++, 75 %
	Acute response	++, 80 %	+++, 90 %	+++, 95 %	+++, 95 %
	Long term effects	+++, 80 %	++, 75 %	+++, 90 %	+++, 75 %
COX IV	Control	+, 5 %	+, 10 %	+, 5 %	++, 25 %
	Acute response	++, 25 %	++,50 %	++, 25 %	++, 50 %
	Long term effects	+,10 %	++, 25 %	++, 50 %	++, 50 %

Note: Intensity of staining: +: weak; ++: moderate; +++: strong; Percentage: 1=<25 %, 2=25–50 %, 3=50–75 %, 4=>75 %. To further examine if the increased mitochondria numbers were maintained for long-term, we examined the mitochondria positivity in the remnant/recurrent xenograft tumors when the animals had to be euthanized due to excessive tumor growth. In both xenograft models, the increased mitochondria were maintained in the invasive foci, whereas in the tumor core mass, the expression of mitochondria was reduced from the peak levels observed immediately at the end of radiation. The overall levels, however, was still higher than that of the non-radiated control. This type of mitochondrial biogenesis, i.e., triggered by fractionated radiation and persisted for long-term *in vivo* in the surviving tumor cells, may have played a role in resisting radiation induced cells death in pHGG.

The elevated mitochondria were functionally activated

Ionizing radiation can cause impaired mitochondrial function through DNA damaging ([45,46]). To further investigate if the increased mitochondria were functional, we examined the expression of mitochondrial respiratory protein cytochrome C oxidase subunit IV (COX IV), a mitochondrial-specific protein that has been reliably used as a functional indicator of mitochondria [47]. Similar to the changes in mitochondria numbers, the protein expression of COX IV was significantly elevated in both the tumor core and invasive fronts in the PDOX tumors at the end of 5-day radiation (2 Gy per day) (Fig. 3B, Table 2). Subsequent analysis of the recurrent tumor showed that the COX IV expression in IC-2305HGG was reduced to a low level comparable to the untreated controls; whereas in the model with DNA MMR deficiency (IC-1406HGG), high expression levels of COX IV were maintained in both tumor core and invasive cells (Fig. 3B, Table 2).

Reactive oxygen species (ROS) were increased following fractionated radiation

ROS are generated as normal products of cellular metabolism ([48,49]). They can also be produced by exogenous sources such as ionizing radiation ([9,50]). Since mitochondria are the major sources of ROS production ([9,51]), we next examined if the increased mitochondria in the pHGG xenograft tumor cells were also correlated with increased ROS production. Through flow cytometric analysis of a cell permeable florescent probe DCF-DA, the most widely used techniques for direct measuring of redox state [52], we detected a right shift of the relative fluorescence peak on a log scaled x-axis in both models 5 days post radiation as compared with the control tumors (Fig. 3C). Taken together, these data suggest that the increased mitochondria were functionally active and correlated with the increase of ROS production.

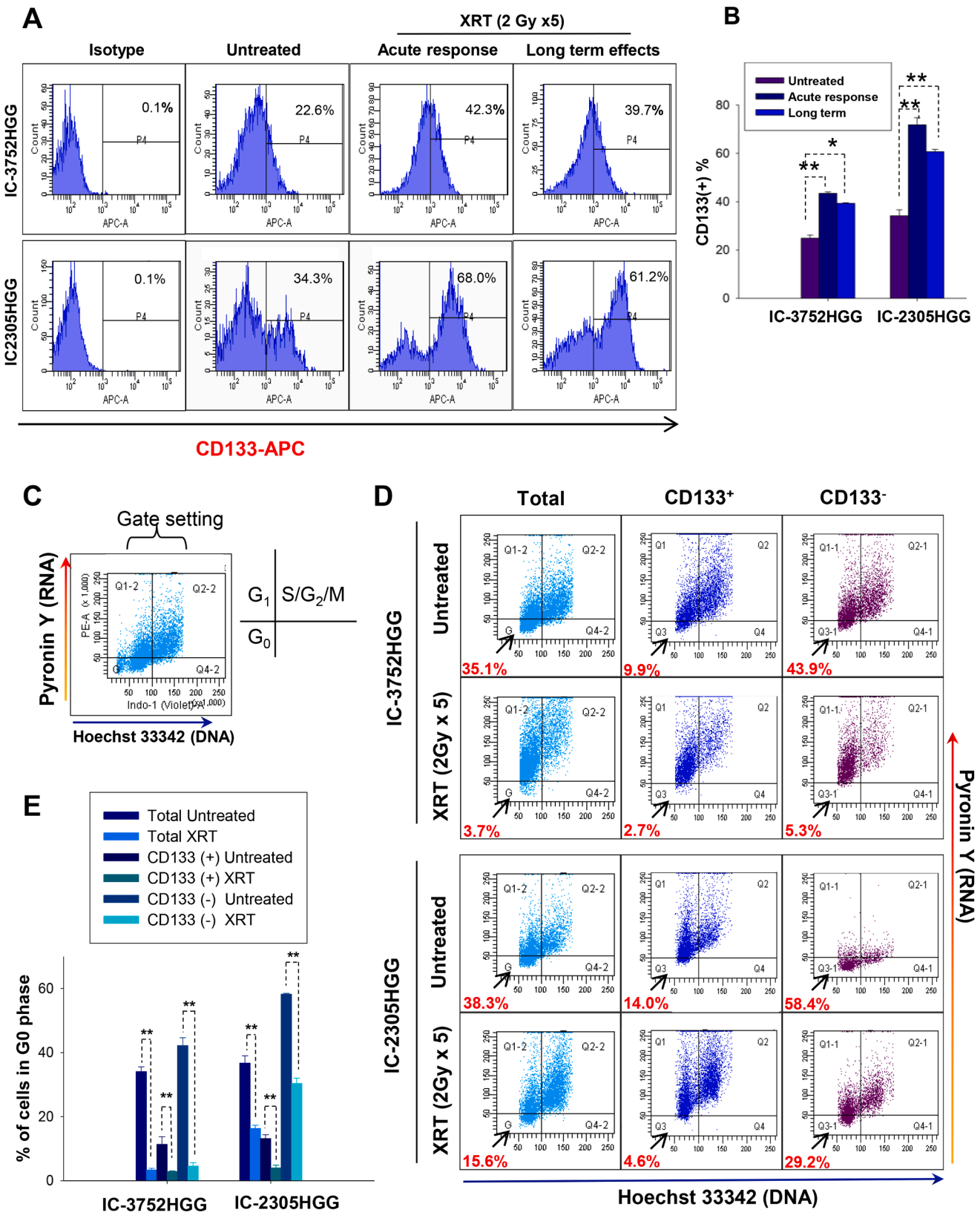

Fig. 4. Flow cytometric analysis of CD133$^+$ and CD133$^-$ tumor cells following fractionated radiation *in vivo*. (A) Flow chart showing the increase of CD133$^+$ glioma cells from the acute response phase and lasted for long-term in the remanent tumors. (B) Quantification of CD133$^+$ glioma cell after fractionated radiation in both mouse model. Data from at least three independent experiments are shown. (C) FCM gate setting for G_0, G_1 and S/G_2M analysis. Tumor cells were sequentially incubated with Hoechst 33342 to stain DNA and Pyronin Y to stain RNA. (D) Representative flow chart showing the reduction of G_0 phase cells accompanied by the increase of G_1 phase cells. Tumor cells were harvested at the end of 5-day radiation (2 Gy per day). (E) Quantification of G_0 cell after fractionated irradiation. Data from at least three independent experiments are shown (Mean ± SD) ($P < 0.01$).

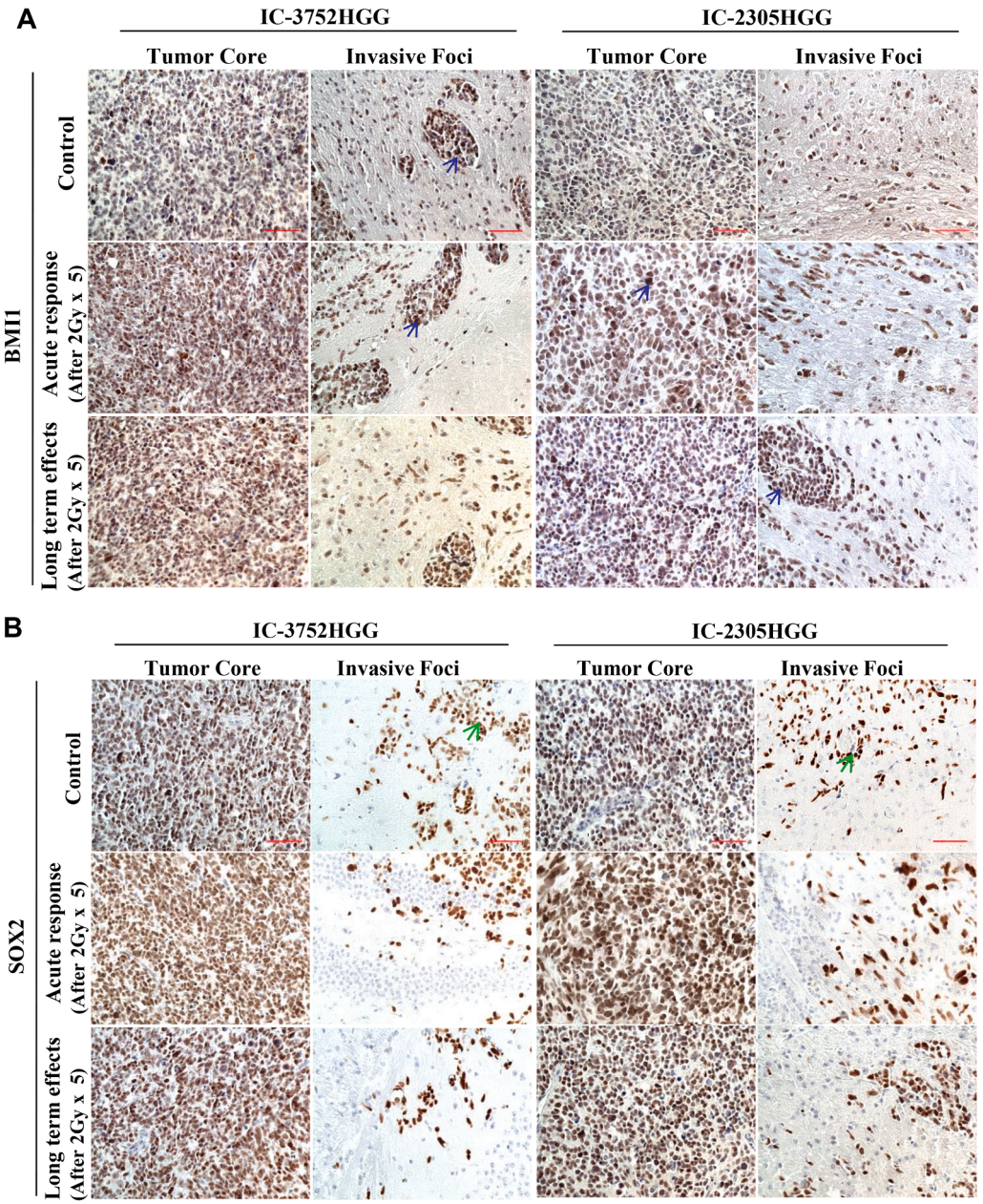

Fig. 5. Representative images of immunohistochemical staining of PDOX tumor cells at the end of acute and long-term radiation therapy in tumor core and invasive front in two pHGG models (IC-3752HGG, IC-2305HGG) (quantification data summarized in Table 3). (A) Nuclear protein expression of BMI1(*blue arrow*). (B) Nuclear protein expression of COX IV (*green arrow*) (*green arrow*). Representative images were from three independent experiments. (Original magnification, 40×10). Bar = 50 μm.

Fractionated radiotherapy increased CD133$^+$ cells in vivo

Cancer stem cells (**CSCs**) are shown to contribute to radio-resistance in adult GBMs ([53,54]). Although it remains controversial about its specificity, CD133 have been widely used as enrichment markers of glioma stem cells (GSCs) ([55,56]). To determine their responses toward fractionated radiotherapy, we examined relative abundances of CD133$^+$ cells with FCM in pHGG orthotopic xenograft tumors immediately at the end of radiation treatment (2 Gy/day for 5 days). In addition to IC-2305HGG, the model IC-3752HGG was prioritized over IC-1406HGG in this assay due to its representation of a common molecular subtypes (MYCN) (one of the three models we have developed) (Table 1), strong resistance to fractionated XRT (Fig. 1B) and rapid *in vivo* growth. In both models, the fractions of CD133$^+$ cells were increased, ranging from 22.6 % ± 1.3 % to 42.3 % ± 0.6 % in IC-3752HGG, and from 34.3 % ± 2.5 % to 66.0 % ± 3.0 % in IC-2305HGG) ($P < 0.05$) (Fig. 4A, B). These data suggested that pHGG CD133$^+$ glioma cells were more resistant to ionizing radiation.

Radiotherapy activates cell cycle entry of quiescent G0 phase tumor cells in vivo

The mechanisms of post-radiation enrichment of CSC remain unclear. We reasoned that it could be caused by the death of CD133$^-$ tumor cells or resulted from the activated proliferation of CD133$^+$ cells, or both. Given the critical roles of quiescence in resisting therapy-induced cell killing, in maintaining self-renewal of CSC and in limiting DNA damage [57], we analyzed the changes of G_0 phase quiescent cells in the two PDOX models using a FCM protocol that can differentiate G_0 from G_1 phase cells by sequential staining of tumor cell DNA with Hoechst

Table 3
Summary of immunohistochemical staining of self-renewal (BMI1 and SOX2).

Gene	Group	IC-3752HGG		IC-2305HGG	
		Tumor Core	Invasive Foci	Tumor Core	Invasive Foci
BMI1	Control	+, 60 %	++,70 %	+, 50 %	++,80 %
	Acute response	+++,100 %	+++,100 %	+++,100 %	+++,100 %
	Long term effects	+++,100 %	+++,100 %	+,100 %	+++,100 %
SOX2	Control	+,90 %	+++,100 %	+,70 %	+++,100 %
	Acute response	+++,100 %	+++,100 %	+++,100 %	+++,100 %
	Long term effects	++,100 %	+++,100 %	++,100 %	+++,100 %

Note: Intensity of staining: +: weak; ++: moderate; +++: strong; Percentage: 1=<25 %, 2=25–50 %, 3=50–75 %, 4=>75 %.

33342 and RNA with Pyronin Y ([58,59]). Compared with the untreated models, radiation (2 Gy/day x 5 days) significantly reduced the total G_0 phase cells from 35.1 % to 3.7 % in IC-3752HGG, and 38.3 % to 15.6 % in IC-2305HGG (Fig. 4D).

Further analysis of the purified $CD133^+$ and $CD133^-$ cells revealed a 3.6-fold (from 9.9 % to 2.7 %) reduction of quiescent $CD133^+$ cells in IC-3752HGG and a 3-fold (from 14 % to 4.5 %) reduction in IC-2305HGG. Similar patterns were noted in $CD133^-$ cells, in which the reduction of G_0 quiescent cells ranged from 8.3 folds (43.9 % to 5.3 %) in IC-3752HGG to 2 folds (58.4 % to 29.2 %) in IC-2305HGG (Figs. 4D, E and S1). These findings are in agreement with the elevated cell proliferation detected by $Ki67^+$ cells in the current study. They do not seem to support the notion that quiescent tumor cells survive fractionated radiation by passively staying at the resting phase. Rather, the tumor cells, particularly the $CD133^+$ CSCs, actively responded to the radiation therapy by exiting quiescence and entering active cell cycling. They have also provided insights, at least partially, for the enrichment and increase of CSCs.

Irradiation upregulates the expression of stem cell self-renewal gene BMI1 and SOX2

BMI1 and SOX2 are important self-renewal genes both in normal and CSCs ([60,61]), and their over-expression have been detected in high-grade gliomas of adults and children [60]. BMI1 has been found to promote DNA double strand break (DSB) response and repair [62]. In the untreated tumors of our PDOX models, we observed BMI1 over-expression, albeit at low levels (+), in ~50-60 % tumor cells and SOX2 in ~90 % tumor cells in the tumor core areas; whereas in the invasive single cells and micro-satellite foci, we detected medium levels (++) of over-expression (Fig. 5A, B, and Table 3), indicating that BMI1 and SOX2 may have participated in glioma cell invasion.

After fractionated radiotherapy, BMI1 and SOX2 expression increased both in staining intensity (++~+++) and in relative abundance (>90 % of cells), immediately at the end of the 5-day radiation (i.e. the acute phase) and persisted till the end of experiment when the animals had to be euthanized due to tumor growth (i.e. the long-term effects) in both models (IC-3752HGG and IC-2305HGG) (Fig. 5A, B, and Table 3). These results indicated the involvement of BMI1 and SOX2 in mediating pHGG responses towards radiation both in tumor core and in the invasive foci. Given their roles in CSC self-renewal, they may have also participated in promoting the entry of $CD133^+$ cells into cell cycle, which justifies additional mechanistic analysis in the near future.

Fractionated radiotherapy enhanced the mesenchymal maker fibronectin

Epithelial-mesenchymal transition (EMT) is involved in CSC biology and in facilitating tumor invasion and metastasis [63–65]. Tumor cell invasion is associated with a mesenchymal feature of pHGG ([65,66]) and can be affected by the ROS levels [67]. Recognizing the critical role of invasive glioma cells in causing tumor recurrence, we next examined the impact of radiation induced ROS elevation on genes (fibronectin and vimentin) involved in EMT [68]. IHC staining revealed significant increase of fibronectin in the invasive foci in IC-3752HGG from medium (++) to strong (+++) positivity both during acute response and in the long-term effects (Fig. 6A and Table 4). The lack of similar response in IC-2305GBM indicated inter-tumoral heterogeneity. Strong (+++) expression of vimentin, another important regulator gene of EMT [65], was detected in both models in >95 % cells, and radiation did not cause major changes in its expression (Fig. 6B and Table 4).

Discussion

In this study, we demonstrated that the administration of clinically relevant and fractionated radiation to PDOX models of pHGG is feasible. The overall response of these orthotopic xenograft tumors parallels patients' response. We showed that fractionated radiation (2 Gy daily for 5 days) caused wide-spread DNA damage both in the invasive cells and in the tumor core area, which resulted in apoptosis and mitotic catastrophe in ~ 30 % of the tumor cells and extended animal survival times. To search for additional mechanisms of radiation resistance, we identified mitochondrial biogenesis and the entry of $CD133^+$ CSCs from quiescent G_0 phase into cell cycle as two new strategies of radiation resistance.

Radio-resistance is one of the major mechanisms of tumor recurrence in pediatric gliomas ([69,54]). However, our understanding of their resistance mechanisms *in vivo* is limited, due to the difficulties of obtaining post-radiation tumor tissues in patients. Our PDOX model have thus provided a unique opportunity to examine the temporal (acute and long-term) and spatial (tumor core vs. invasive foci) responses of pHGGs *in vivo* in a setting that shares maximum similarities to human pHGGs. Additionally, our inclusion of a PDOX model with DNA MMR deficiency, which is shown to be involved in DNA damage recognition, cell cycle arrest, DNA repair and apoptosis [70], further help elucidate the role of radiation induced DNA damage and repair in therapy efficacy. By comparing the responses of xenograft models with and without DNA MMR deficiency, the likelihood of identifying new mechanisms of radio-resistance and post-radiation survival was increased.

Genomic DNA is shown to be the most important subcellular target of radiation therapy and examination of DNA breaks is frequently used as an indicator of radiation-induced cell damage. Successful completion of DNA repair is one of the major mechanisms of cell survival [9]. Many efforts have thus been invested to develop new agents, such as PARP inhibitors, to suppress DNA repair ([71,72]). In this study, we showed that a fractionated radiation (2 Gy daily for 5 days) can indeed cause widespread DNA damages *in vivo* as evidenced by strong positivity of γH2AX, and led to apoptotic or mitotic catastrophic cell death in ~30 % tumor cells. While IHC detection of rH2X provided high (single cell) resolution and spatial distribution of tumor cells suffering DNA damage, additional assays on DNA damage and repair should further strengthen the data and conclusions. While our findings demonstrated the power of fractionated radiation in causing massive DNA damages, they also showed that many tumor cells (~70 %) developed additional strategies to survive despite severe DNA breaks *in vivo*.

Our finding of elevated mitochondria in the surviving pHGG cells suggested a new mechanism of pHGG radio-resistance. Indeed, several recent studies have examined the mitochondrial dysfunction as it related to radiation sensitivities ([11,73,74]). Since the increased levels of mitochondria occurred at the end of the 5-day radiation (the acute phase reaction) and persisted in the remnant tumors (the long-term effect) in both models and were functionally active, new strategies blocking mitochondrial biogenesis and/or inhibiting COX IV over-expression can be tested to reverse radio-resistance in pHGG cells.

Cellular quiescence has long been recognized as one of the important

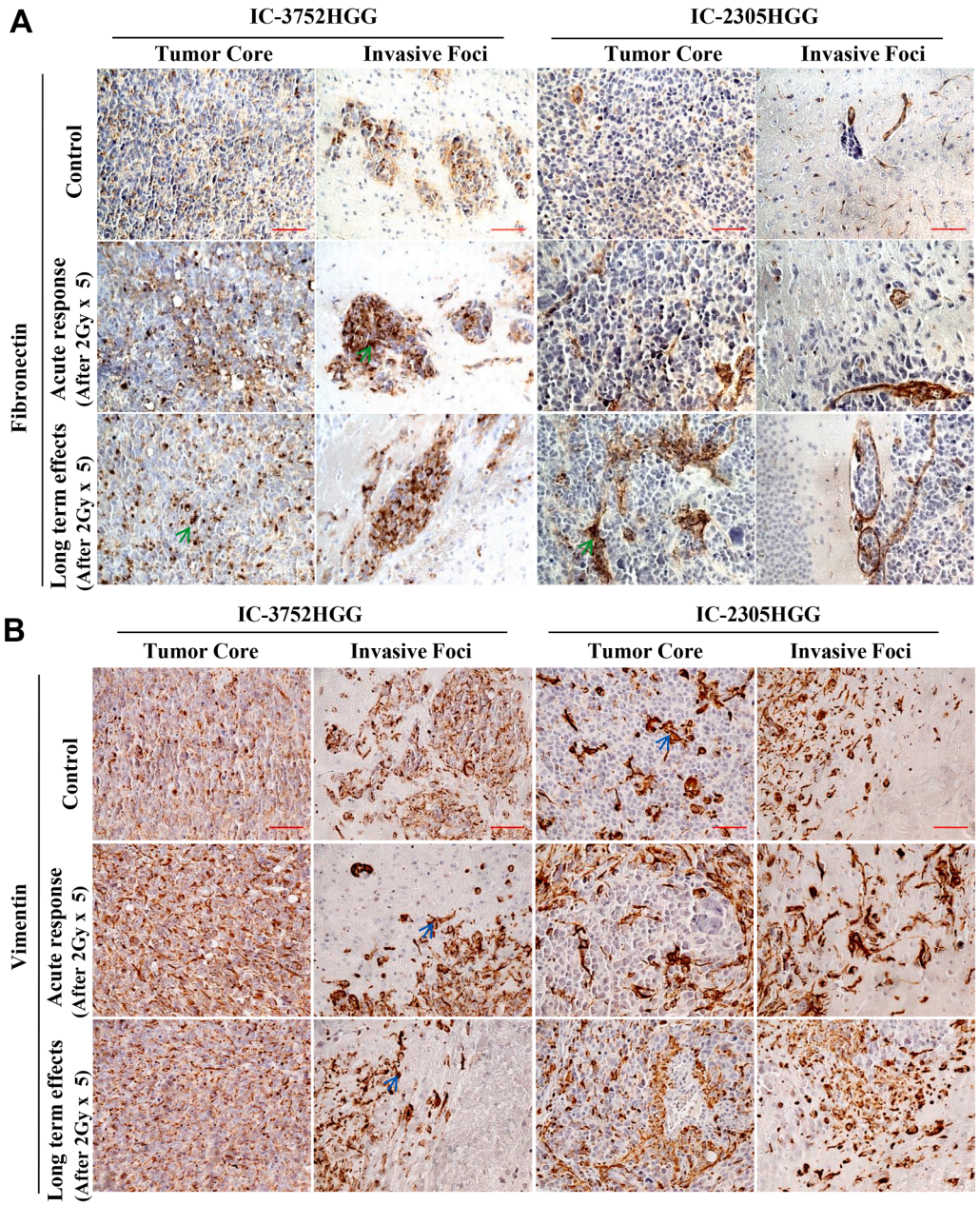

Fig. 6. Representative images of immunohistochemical staining of PDOX tumor cells at the end of acute and long term radiation therapy in both tumor core and invasive front in two pHGG models (IC-3752HGG, IC-2305HGG). (quantification data summarized in Table 4) (A) Cytoplasmic protein expression of Fibronectin (*green arrow*). (B) Cytoplasmic protein expression of Vimentin (*blue arrow*). Representative images were from three independent experiments. (Original magnification, 40×10). Bar = 50 μm.

mechanisms of therapy resistance ([75,76]). This is especially true for the putative CSCs [76–78]. However, the fate of quiescent tumor cells, particularly CSCs, following radiation remains poorly understood. Using our PDOX models that better replicated the microenvironment of pHGG and the maintenance of cellular quiescence, we discovered rapid exit of $CD133^+$ tumor cells from G_0 phase quiescence and into cell cycle progression. This finding was further supported by the significant increase of Ki-67^+ tumor cells detected via immunohistochemical staining. This result is important as it demonstrated a mechanistic rationale for the combination of radiation with cell-cycle specific chemotherapies or target therapies. Additionally, our identification of two self-renewal genes BMI1 and SOX2 as the key molecular drivers of the activated cell cycle entry also provided a mechanism not only to explain the accumulation of CSCs after radiation therapy ([53,54]) but also to combine BMI1 inhibitor with radiation for cancer therapies.

One added advantage of our studies using PDOX models is that we can analyze spatial differences of pHGG cells *in vivo*. Diffuse invasion is a biological hallmark of high-grade gliomas and represent one of the primary causes of tumor recurrence. Our previous studies have revealed significant differences of gene expression and microRNA profiles between GBM cells located in the tumor core and in the invasive front [79]. In the current study, our findings on their mitochondria content extended our knowledge on the biological differences of these two closely related subpopulations. The newly identified differences of energy production between tumor core and invasive glioma cells highlighted the need of in-depth analysis of the mechanistic causes, particularly the enriched mitochondria expression in the invasive cells. It also suggests that future evaluation of therapies should take the spatially located glioma cells into account. All these efforts should inform future development of anti-metabolism and/or anti-invasive

Table 4
Summary of immunohistochemical staining of self-renewal (Fibronectin and Vimentin).

Gene	Group	IC-3752HGG		IC-2305HGG	
		Tumor Core	Invasive Foci	Tumor Core	Invasive Foci
Fibronectin	Control	+,20 %	++, 80 %	++,5 %	+++,10 %
	Acute response	+++,60 %	+++,95 %	+++,30 %	+++,20 %
	Long term effects	+++,70 %	+++,100 %	+++,40 %	+++,25 %
Vimentin	Control	++,90 %	+++,100 %	+++,40 %	+++,100 %
	Acute response	+++,100 %	+++,100 %	+++,60 %	+++,100 %
	Long term effects	++,100 %	+++,100 %	+++,80 %	+++,100 %

Note: Intensity of staining: +: weak; ++: moderate; +++: strong; Percentage: 1=<25 %, 2=25–50 %, 3=50–75 %, 4=>75 %.

therapies against HGGs

Conclusions

Our study demonstrated that clinically relevant fractionated radiation therapy can be successfully administered to PDOX models of pHGG. We confirmed that the five-day fractionated radiation was effective in causing widespread DNA damages *in vivo* although improvement of animal survival times was less than expected. We identified two new mechanisms, i.e., mitochondrial biogenesis and activation of cell cycle progression, with which pHGG cells develop resistance to radiation induced cell death. More importantly, our data suggested new therapeutic strategies to overcome radio-resistance and ultimately to improve therapy efficacy of radiation in pHGGs.

Funding

This work was funded by the NIH/NCI RO1 CA185402 (Li XN), Guangdong Basic and Applied Basic Research Foundation (No. 2021A1515010416, Liu ZG), Dongguan Science and Technology of Social Development Program (No. 20231800900382, Liu ZG), St. Baldrick's Foundation (Grant 2532341503, Su JM), Golfers against Cancer (Li XN), Childhood brain tumor foundation (Li XN), National Brain Tumor Foundation (Li XN), The Science Development Program of Guangzhou 201707020001(Xia YF).

Ethics approval and consent to participate

The study was conducted in accordance with the Declaration of Helsinki, and approved by the Institutional Review Board of Baylor College of Medicine (H-4844) for studies involving humans. The animal study was performed by following Institutional Animal Care and Use Committee (IACUC) approved protocol (AN-4548) at Baylor College of Medicine and IS00009226 at Northwestern University.

Availability of data and materials

The datasets used and/or analysed during the current study are available from the corresponding author on reasonable request.

Informed consent statement

Informed consent was obtained from all subjects involved in the study.

Supplementary

Supplementary Fig. 1. Radiotherapy drove G_0 cells to G_1 phase both in $CD133^+$ and $CD133^-$ live glioma cells *in vivo*.

CRediT authorship contribution statement

Zi-Lu Huang: Writing – review & editing, Validation, Formal analysis, Data curation. **Zhi-Gang Liu:** Writing – original draft, Validation, Methodology, Formal analysis, Data curation, Conceptualization. **Qi Lin:** Methodology. **Ya-Lan Tao:** Methodology. **Xinzhuoyun Li:** Writing – review & editing. **Patricia Baxter:** Resources. **Jack MF Su:** Resources, Funding acquisition. **Adekunle M. Adesina:** Formal analysis. **Chris Man:** Data curation. **Murali Chintagumpala:** Resources. **Wan Yee Teo:** Writing – original draft. **Yu-Chen Du:** Validation, Supervision, Project administration. **Yun-Fei Xia:** Supervision, Funding acquisition, Conceptualization. **Xiao-Nan Li:** Writing – review & editing, Writing – original draft, Supervision, Funding acquisition, Formal analysis, Conceptualization.

Declaration of competing interest

The authors declare that they have no known competing financial interests or personal relationships that could have appeared to influence the work reported in this paper.

Acknowledgment

Not applicable.

Supplementary materials

Supplementary material associated with this article can be found, in the online version, at doi:10.1016/j.tranon.2024.101988.

References

[1] C. Erker, B. Tamrazi, T.Y. Poussaint, S. Mueller, D. Mata-Mbemba, E. Franceschi, et al., Response assessment in paediatric high-grade glioma: recommendations from the Response Assessment in Pediatric Neuro-Oncology (RAPNO) working group, Lancet Oncol. 21 (6) (2020) e317–ee29.
[2] C. Jones, M.A. Karajannis, D.T.W. Jones, M.W. Kieran, M. Monje, S.J. Baker, et al., Pediatric high-grade glioma: biologically and clinically in need of new thinking, Neuro Oncol. 19 (2) (2017) 153–161.
[3] D. Sturm, S.M. Pfister, D.T.W. Jones, Pediatric gliomas: current concepts on diagnosis, biology, and clinical management, J. Clin. Oncol. 35 (21) (2017) 2370–2377.
[4] N. Gaspar, L. Marshall, L. Perryman, D.A. Bax, S.E. Little, M. Viana-Pereira, et al., MGMT-independent temozolomide resistance in pediatric glioblastoma cells associated with a PI3-kinase-mediated HOX/stem cell gene signature, Cancer Res. 70 (22) (2010) 9243–9252.
[5] R.I. Jakacki, K.J. Cohen, A. Buxton, M.D. Krailo, P.C. Burger, M.K. Rosenblum, et al., Phase 2 study of concurrent radiotherapy and temozolomide followed by temozolomide and lomustine in the treatment of children with high-grade glioma: a report of the Children's Oncology Group ACNS0423 study, Neuro Oncol. 18 (10) (2016) 1442–1450.
[6] A. Korshunov, M. Ryzhova, V. Hovestadt, S. Bender, D. Sturm, D. Capper, et al., Integrated analysis of pediatric glioblastoma reveals a subset of biologically favorable tumors with associated molecular prognostic markers, Acta Neuropathol. 129 (5) (2015) 669–678.
[7] J. DeSisto, J.T. Lucas Jr., K. Xu, A. Donson, T. Lin, B. Sanford, et al., Comprehensive molecular characterization of pediatric radiation-induced high-grade glioma, Nat. Commun. 12 (1) (2021) 5531.
[8] T. Helleday, E. Petermann, C. Lundin, B. Hodgson, RA. Sharma, DNA repair pathways as targets for cancer therapy, Nat. Rev. Cancer 8 (3) (2008) 193–204.
[9] K. Valerie, A. Yacoub, M.P. Hagan, D.T. Curiel, P.B. Fisher, S. Grant, et al., Radiation-induced cell signaling: inside-out and outside-in, Mol. Cancer Ther. 6 (3) (2007) 789–801.
[10] D.R. Green, G. Kroemer, The pathophysiology of mitochondrial cell death, Science 305 (5684) (2004) 626–629 (1979).
[11] D. Averbeck, C. Rodriguez-Lafrasse, Role of Mitochondria in Radiation Responses: Epigenetic, Metabolic, and Signaling Impacts, Int. J. Mol. Sci. 22 (20) (2021).
[12] N.H. Boyd, A.N. Tran, J.D. Bernstock, T. Etminan, A.B. Jones, G.Y. Gillespie, et al., Glioma stem cells and their roles within the hypoxic tumor microenvironment, Theranostics 11 (2) (2021) 665–683.

[13] M. Abdouh, S. Facchino, W. Chatoo, V. Balasingam, J. Ferreira, G. Bernier, BMI1 sustains human glioblastoma multiforme stem cell renewal, J. Neurosci. 29 (28) (2009) 8884–8896.
[14] R.M. Gangemi, F. Griffero, D. Marubbi, M. Perera, M.C. Capra, P. Malatesta, et al., SOX2 silencing in glioblastoma tumor-initiating cells causes stop of proliferation and loss of tumorigenicity, Stem Cells 27 (1) (2009) 40–48 (1981).
[15] M. Diehn, R.W. Cho, N.A. Lobo, T. Kalisky, M.J. Dorie, A.N. Kulp, et al., Association of reactive oxygen species levels and radioresistance in cancer stem cells, Nature 458 (7239) (2009) 780–783.
[16] F. Pajonk, E. Vlashi, WH. McBride, Radiation resistance of cancer stem cells: the 4 R's of radiobiology revisited, Stem Cells 28 (4) (2010) 639–648 (1981).
[17] M. Jamal, B.H. Rath, E.S. Williams, K. Camphausen, PJ. Tofilon, Microenvironmental regulation of glioblastoma radioresponse, Clin. Cancer Res. 16 (24) (2010) 6049–6059.
[18] Q. Shu, K.K. Wong, J.M. Su, A.M. Adesina, L.T. Yu, Y.T. Tsang, et al., Direct orthotopic transplantation of fresh surgical specimen preserves CD133+ tumor cells in clinically relevant mouse models of medulloblastoma and glioma, Stem Cells 26 (6) (2008) 1414–1424 (1981).
[19] L. Yu, P.A. Baxter, H. Voicu, S. Gurusiddappa, Y. Zhao, A. Adesina, et al., A clinically relevant orthotopic xenograft model of ependymoma that maintains the genomic signature of the primary tumor and preserves cancer stem cells *in vivo*, Neuro Oncol. 12 (6) (2010) 580–594.
[20] J.L. Rokita, K.S. Rathi, M.F. Cardenas, K.A. Upton, J. Jayaseelan, K.L. Cross, et al., Genomic profiling of childhood tumor patient-derived xenograft models to enable rational clinical trial design, Cell Rep. 29 (6) (2019) 1675. -89.e9.
[21] S.R. Hamilton, B. Liu, R.E. Parsons, N. Papadopoulos, J. Jen, S.M. Powell, et al., The molecular basis of Turcot's syndrome, N. Engl. J. Med. 332 (13) (1995) 839–847.
[22] N.C. Nicolaides, N. Papadopoulos, B. Liu, Y.F. Wei, K.C. Carter, S.M. Ruben, et al., Mutations of two PMS homologues in hereditary nonpolyposis colon cancer, Nature 371 (6492) (1994) 75–80.
[23] L. Huang, S. Garrett Injac, K. Cui, F. Braun, Q. Lin, Y. Du, et al., Systems biology-based drug repositioning identifies digoxin as a potential therapy for groups 3 and 4 medulloblastoma, Sci. Transl. Med. 10 (464) (2018) 465.
[24] L. Qi, H. Lindsay, M. Kogiso, Y. Du, F.K. Braun, H. Zhang, et al., Evaluation of an EZH2 inhibitor in patient-derived orthotopic xenograft models of pediatric brain tumors alone and in combination with chemo- and radiation therapies, Lab. Investig. 102 (2) (2022) 185–193.
[25] Q. Shu, B. Antalffy, J.M. Su, A. Adesina, C.N. Ou, T. Pietsch, et al., Valproic Acid prolongs survival time of severe combined immunodeficient mice bearing intracerebellar orthotopic medulloblastoma xenografts, Clin. Cancer Res. 12 (15) (2006) 4687–4694.
[26] Z. Liu, X. Zhao, H. Mao, P.A. Baxter, Y. Huang, L. Yu, et al., Intravenous injection of oncolytic picornavirus SVV-001 prolongs animal survival in a panel of primary tumor-based orthotopic xenograft mouse models of pediatric glioma, Neuro Oncol. 15 (9) (2013) 1173–1185.
[27] L. Yu, P.A. Baxter, X. Zhao, Z. Liu, L. Wadhwa, Y. Zhang, et al., A single intravenous injection of oncolytic picornavirus SVV-001 eliminates medulloblastomas in primary tumor-based orthotopic xenograft mouse models, Neuro Oncol. 13 (1) (2010) 14–27.
[28] H. Zhang, Y. Du, L. Qi, S. Xiao, F.K. Braun, M. Kogiso, et al., Targeting GBM with an oncolytic picornavirus SVV-001 alone and in combination with fractionated Radiation in a Novel Panel of Orthotopic PDX models, J. Transl. Med. 21 (1) (2023) 444.
[29] M. Kogiso, L. Qi, F.K. Braun, S.G. Injac, L. Zhang, Y. Du, et al., Concurrent inhibition of neurosphere and monolayer cells of pediatric glioblastoma by Aurora A inhibitor MLN8237 predicted survival extension in PDOX Models, Clin. Cancer Res. 24 (9) (2018) 2159–2170.
[30] M. Kogiso, L. Qi, Y. Du, F.K. Braun, H. Zhang, L.F. Huang, et al., Synergistic anti-tumor efficacy of mutant isocitrate dehydrogenase 1 inhibitor SYC-435 with standard therapy in patient-derived xenograft mouse models of glioma, Transl. Oncol. 18 (2022) 101368.
[31] C.S. Grasso, Y. Tang, N. Truffaux, N.E. Berlow, L. Liu, M.A. Debily, et al., Functionally defined therapeutic targets in diffuse intrinsic pontine glioma, Nat. Med. 21 (6) (2015) 555–559.
[32] M. Kioi, H. Vogel, G. Schultz, R.M. Hoffman, G.R. Harsh, J.M. Brown, Inhibition of vasculogenesis, but not angiogenesis, prevents the recurrence of glioblastoma after irradiation in mice, J. Clin. Investig. 120 (3) (2010) 694–705.
[33] L. Qi, M. Kogiso, Y. Du, H. Zhang, F.K. Braun, Y. Huang, et al., Impact of SCID mouse gender on tumorigenicity, xenograft growth and drug-response in a large panel of orthotopic PDX models of pediatric brain tumors, Cancer Lett. 493 (2020) 197–206.
[34] X. Zhao, Y.J. Zhao, Q. Lin, L. Yu, Z. Liu, H. Lindsay, et al., Cytogenetic landscape of paired neurospheres and traditional monolayer cultures in pediatric malignant brain tumors, Neuro Oncol. 17 (7) (2015) 965–977.
[35] E.P. Rogakou, D.R. Pilch, A.H. Orr, V.S. Ivanova, WM. Bonner, DNA double-stranded breaks induce histone H2AX phosphorylation on serine 139, J. Biol. Chem. 273 (10) (1998) 5858–5868.
[36] S. Burma, B.P. Chen, M. Murphy, A. Kurimasa, DJ. Chen, ATM phosphorylates histone H2AX in response to DNA double-strand breaks, J. Biol. Chem. 276 (45) (2001) 42462–42467.
[37] D.B. Hoelzinger, T. Demuth, ME. Berens, Autocrine factors that sustain glioma invasion and paracrine biology in the brain microenvironment, J. Natl. Cancer Inst. 99 (21) (2007) 1583–1593.
[38] H. Vakifahmetoglu, M. Olsson, B. Zhivotovsky, Death through a tragedy: mitotic catastrophe, Cell Death Differ. 15 (7) (2008) 1153–1162.
[39] J. Gliemroth, T. Feyerabend, C. Gerlach, H. Arnold, AJ. Terzis, Proliferation, migration, and invasion of human glioma cells exposed to fractionated radiotherapy *in vitro*, Neurosurg. Rev. 26 (3) (2003) 198–205.
[40] K.W. Kim, L. Moretti, L.R. Mitchell, D.K. Jung, B. Lu, Combined Bcl-2/mammalian target of rapamycin inhibition leads to enhanced radiosensitization via induction of apoptosis and autophagy in non-small cell lung tumor xenograft model, Clin. Cancer Res. 15 (19) (2009) 6096–6105.
[41] K.H. Higuchi, T. Nakano, A. Tsuboi, Y. Suzuki, T. Ohno, K. Oka, Flow cytometric and Ki-67 immunohistochemical analysis of cell cycle distribution of cervical cancer during radiation therapy, Anticancer Res. 21 (4A) (2001) 2511–2518.
[42] T. Takahashi, T. Nakano, K. Oka, K. Ando, Transitional increase in growth fraction estimated by Ki-67 index after irradiation to human tumor in xenograft, Anticancer Res. 24 (1) (2004) 107–110.
[43] L.E. Broker, F.A. Kruyt, G. Giaccone, Cell death independent of caspases: a review, Clin. Cancer Res. 11 (9) (2005) 3155–3162.
[44] J. Kluza, P. Marchetti, M.A. Gallego, S. Lancel, C. Fournier, A. Loyens, et al., Mitochondrial proliferation during apoptosis induced by anticancer agents: effects of doxorubicin and mitoxantrone on cancer and cardiac cells, Oncogene 23 (42) (2004) 7018–7030.
[45] Z. Li, A.H. Pearlman, P. Hsieh, DNA mismatch repair and the DNA damage response, DNa Repair 38 (2016) 94–101 (Amst).
[46] S.P. Jackson, J. Bartek, The DNA-damage response in human biology and disease, Nature 461 (7267) (2009) 1071–1078.
[47] Y. Li, J.S. Park, J.H. Deng, Y. Bai, Cytochrome c oxidase subunit IV is essential for assembly and respiratory function of the enzyme complex, J. Bioenerg. Biomembr. 38 (5-6) (2006) 283–291.
[48] P.R. Angelova, AY. Abramov, Role of mitochondrial ROS in the brain: from physiology to neurodegeneration, FEBS Lett. 592 (5) (2018) 692–702.
[49] F.L. Muller, Y. Liu, M.A. Abdul-Ghani, M.S. Lustgarten, A. Bhattacharya, Y.C. Jang, et al., High rates of superoxide production in skeletal-muscle mitochondria respiring on both complex I- and complex II-linked substrates, Biochem. J. 409 (2) (2008) 491–499.
[50] C. Du, Z. Gao, V.A. Venkatesha, A.L. Kalen, L. Chaudhuri, D.R. Spitz, et al., Mitochondrial ROS and radiation induced transformation in mouse embryonic fibroblasts, Cancer Biol. Ther. 8 (20) (2009) 1962–1971.
[51] D. Han, E. Williams, E. Cadenas, Mitochondrial respiratory chain-dependent generation of superoxide anion and its release into the intermembrane space, Biochem. J. 353 (Pt 2) (2001) 411–416.
[52] M. Degli Esposti, Measuring mitochondrial reactive oxygen species, Methods 26 (4) (2002) 335–340.
[53] D. Hambardzumyan, M. Squatrito, EC. Holland, Radiation resistance and stem-like cells in brain tumors, Cancer Cell 10 (6) (2006) 454–456.
[54] S. Bao, Q. Wu, R.E. McLendon, Y. Hao, Q. Shi, A.B. Hjelmeland, et al., Glioma stem cells promote radioresistance by preferential activation of the DNA damage response, Nature 444 (7120) (2006) 756–760.
[55] V.V. Hira, K.J. Ploegmakers, F. Grevers, U. Verbovsek, C. Silvestre-Roig, E. Aronica, et al., CD133+ and Nestin+ glioma stem-like cells reside around CD31 + arterioles in niches that express SDF-1alpha, CXCR4, osteopontin and cathepsin K, J. Histochem. Cytochem. 63 (7) (2015) 481–493.
[56] K. Holmberg Olausson, C.L. Maire, S. Haidar, J. Ling, E. Learner, M. Nister, et al., Prominin-1 (CD133) defines both stem and non-stem cell populations in CNS development and gliomas, PLoS One 9 (9) (2014) e106694.
[57] A. Viale, F. De Franco, A. Orleth, V. Cambiaghi, V. Giuliani, D. Bossi, et al., Cell-cycle restriction limits DNA damage and maintains self-renewal of leukaemia stem cells, Nature 457 (7225) (2009) 51–56.
[58] H. Glimm, I.H. Oh, CJ. Eaves, Human hematopoietic stem cells stimulated to proliferate *in vitro* lose engraftment potential during their S/G(2)/M transit and do not reenter G(0), Blood 96 (13) (2000) 4185–4193.
[59] HM. Shapiro, Flow cytometric estimation of DNA and RNA content in intact cells stained with Hoechst 33342 and pyronin Y, Cytometry 2 (3) (1981) 143–150.
[60] P.A. Baxter, Q. Lin, H. Mao, M. Kogiso, X. Zhao, Z. Liu, et al., Silencing BMI1 eliminates tumor formation of pediatric glioma CD133+ cells not by affecting known targets but by down-regulating a novel set of core genes, Acta Neuropathol. Commun. 2 (2014) 160.
[61] P. Ellis, B.M. Fagan, S.T. Magness, S. Hutton, O. Taranova, S. Hayashi, et al., SOX2, a persistent marker for multipotential neural stem cells derived from embryonic stem cells, the embryo or the adult, Dev. Neurosci. 26 (2-4) (2004) 148–165.
[62] S. Facchino, M. Abdouh, W. Chatoo, G. Bernier, BMI1 confers radioresistance to normal and cancerous neural stem cells through recruitment of the DNA damage response machinery, J. Neurosci. 30 (30) (2010) 10096–10111.
[63] Y. Katsuno, R. Derynck, Epithelial plasticity, epithelial-mesenchymal transition, and the TGF-beta family, Dev. Cell 56 (6) (2021) 726–746.
[64] J. Yang, P. Antin, G. Berx, C. Blanpain, T. Brabletz, M. Bronner, et al., Guidelines and definitions for research on epithelial-mesenchymal transition, Nat. Rev. Mol. Cell Biol. 21 (6) (2020) 341–352.
[65] U.D. Kahlert, G. Nikkhah, J. Maciaczyk, Epithelial-to-mesenchymal(-like) transition as a relevant molecular event in malignant gliomas, Cancer Lett. 331 (2) (2013) 131–138.
[66] A. Flamier, M. Abdouh, R. Hamam, A. Barabino, N. Patel, A. Gao, et al., Off-target effect of the BMI1 inhibitor PTC596 drives epithelial-mesenchymal transition in glioblastoma multiforme, npj Precis. Oncol. 4 (2020) 1.
[67] J.K. Lee, K.M. Joo, J. Lee, Y. Yoon, DH. Nam, Targeting the epithelial to mesenchymal transition in glioblastoma: the emerging role of MET signaling, OncoTargets Ther. 7 (2014) 1933–1944.
[68] E. Serres, F. Debarbieux, F. Stanchi, L. Maggiorella, D. Grall, L. Turchi, et al., Fibronectin expression in glioblastomas promotes cell cohesion, collective invasion

of basement membrane *in vitro* and orthotopic tumor growth in mice, Oncogene 33 (26) (2014) 3451–3462.
[69] S. Mueller, S. Chang, Pediatric brain tumors: current treatment strategies and future therapeutic approaches, Neurotherapeutics 6 (3) (2009) 570–586.
[70] S.A. Martin, C.J. Lord, A. Ashworth, Therapeutic targeting of the DNA mismatch repair pathway, Clin. Cancer Res. 16 (21) (2010) 5107–5113.
[71] H.D. Thomas, C.R. Calabrese, M.A. Batey, S. Canan, Z. Hostomsky, S. Kyle, et al., Preclinical selection of a novel poly(ADP-ribose) polymerase inhibitor for clinical trial, Mol. Cancer Ther. 6 (3) (2007) 945–956.
[72] A.L. Russo, H.C. Kwon, W.E. Burgan, D. Carter, K. Beam, X. Weizheng, et al., *In vitro* and *in vivo* radiosensitization of glioblastoma cells by the poly (ADP-ribose) polymerase inhibitor E7016, Clin. Cancer Res. 15 (2) (2009) 607–612.
[73] T. Yamazaki, A. Kirchmair, A. Sato, A. Buque, M. Rybstein, G. Petroni, et al., Mitochondrial DNA drives abscopal responses to radiation that are inhibited by autophagy, Nat. Immunol. 21 (10) (2020) 1160–1171.
[74] T. Shimura, Mitochondrial signaling pathways associated with DNA damage responses, Int. J. Mol. Sci. 24 (7) (2023) 6128.
[75] F. Francescangeli, M.L. De Angelis, R. Rossi, A. Cuccu, A. Giuliani, R. De Maria, et al., Dormancy, stemness, and therapy resistance: interconnected players in cancer evolution, Cancer Metastasis Rev. 42 (1) (2023) 197–215.
[76] A. Menegakis, R. Klompmaker, C. Vennin, A. Arbusa, M. Damen, B. van den Broek, et al., Resistance of hypoxic cells to ionizing radiation is mediated in part via hypoxia-induced quiescence, Cells 10 (3) (2021) 610.
[77] Y. Iranmanesh, B. Jiang, O.C. Favour, Z. Dou, J. Wu, J. Li, et al., Mitochondria's role in the maintenance of cancer stem cells in glioblastoma, Front. Oncol. 11 (2021) 582694.
[78] C.R. Arnold, J. Mangesius, I.I. Skvortsova, U. Ganswindt, The role of cancer stem cells in radiation resistance, Front. Oncol. 10 (2020) 164.
[79] Y. Huang, L. Qi, M. Kogiso, Y. Du, F.K. Braun, H. Zhang, et al., Spatial dissection of invasive front from tumor mass enables discovery of novel microRNA drivers of glioblastoma invasion, Adv. Sci. 8 (23) (2021) e2101923 (Weinh).